CHAPTER 1
INTRODUCTION

1.1 Background of Study

Thermal cracking of hydrocarbons is an endothermic process that takes place in tubular reactor coils suspended in large gas-fired furnaces. In general, the fuel gas, burned in long flame burners in the bottom of the furnace or in radiation burners in the sidewalls of the furnace, are equally distributed over all burners in the furnace.

In OPTIMAL Furnace case study, the tube coil inside the OPTIMAL Furnace firebox (Furnace 4) have significant bend towards the refractory wall. This is may due to the non uniform of heat distribution towards tube coil inside the firebox. Following are the consequence assumption made due to the bend:

1. Non uniform heat distribution inside Furnace Firebox
2. Difference temperature profile at the tube coil
3. Thermal stresses at certain place on the tube Coil
4. Non uniform phase of thermal expansion
5. Eventually tube coil will bend to the heat source

Therefore, it is suspected because of the non-uniform heat distribution act on the tube coil contribute for the coil to bend near the heat source. In most cases there would be a combination of factors, which ultimately lead to the failure, but this study will be more focus on heat distribution inside the firebox.

1.2 Problem Statement

The study of the heat distribution inside the furnace is an ongoing effort to improve efficiency and reduce cost of the heating. The heat distribution inside the furnace is the main factor contributes to the performance and efficiency of a furnace. A problem will occur such as tube coil bend, if the heat distribution inside the furnace is not uniform. Therefore, it is important to study on the temperature distribution behavior inside the furnace. Hence, this project is to simulate to study the characteristic of heat distribution inside the furnace firebox near the tube coil by taking OPTIMAL Chemical Sdn. Bhd. operating furnace as the case study furnace. (Specifically, Furnace 4, which has a significant problem of tube coil bends).
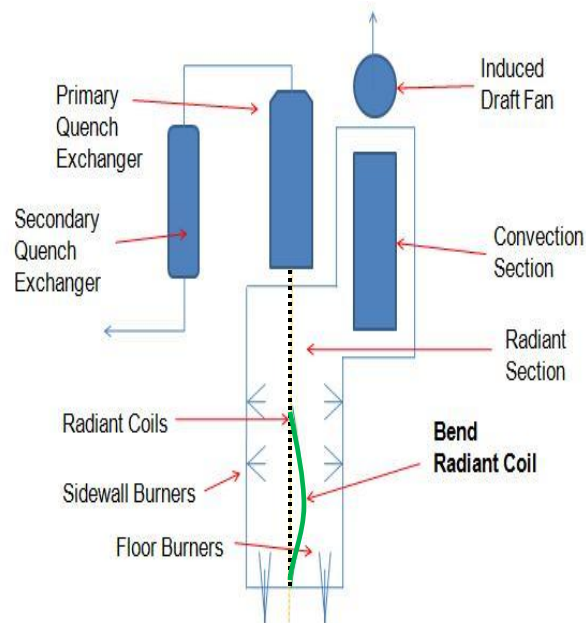

Figure 1 Schematic Diagram of Bent Tube Coil

1.3 Objectives and Scope of Study

The objectives of this project are:

i. To construct a model of the heat distribution inside a furnace firebox by using Gambit Software.

ii. To carry out simulation of the model in Fluent Software.

iii. To validate the model by using the OPTIMAL Chemicals (M) Sdn Bhd operating furnace.

The scope of study can be classified as follow:

- Study on the furnace design of the case study.

- Construct and develop a simulation of heat distribution near the tube coil inside the furnace. The simulation model geometry is designed in simplified geometry, which is enough to cover the intended objectives. The $k - \varepsilon$ are used as closure equations and standards value for constants are adopted. The state of the overall process is considered a steady state process.

- Compare and analyze the model with the operating industrial furnace collected data at the site.

CHAPTER 2
LITERATURE REVIEW

2.1 Steam Cracking Furnace

Furnace[14] is an enclosed chamber in which heat is liberated and transferred directly or indirectly to a solid or fluid mass for the purpose of effecting a physical or chemical change. In OPTIMAL, they are used for steam cracking process[13] for breaking down alkenes (olefins) to simple and light product, which are ethylene and propylene. In steam cracking, ethane and propane (which is what OPTIMAL is processing) is diluted with steam and briefly heated in a furnace without the presence of oxygen. Typically, the cracking reaction temperature is very high, at around 1123°K, but the reaction is only allowed to take place very briefly (0.1s – 0.5s). After the cracking reaction temperature has been reached, the gas is quickly quenched to stop the reaction in a transfer line heat exchanger. Since the process is at high temperature for a long time duration, there may have some failure such as non-uniform heat distribution due to flame impingement, high stress, coke accumulation in the tube coil causes uneven material heating temperature and creep deformation (tendency of a solid material to slowly move or permanently deform under long-term influence of stresses).
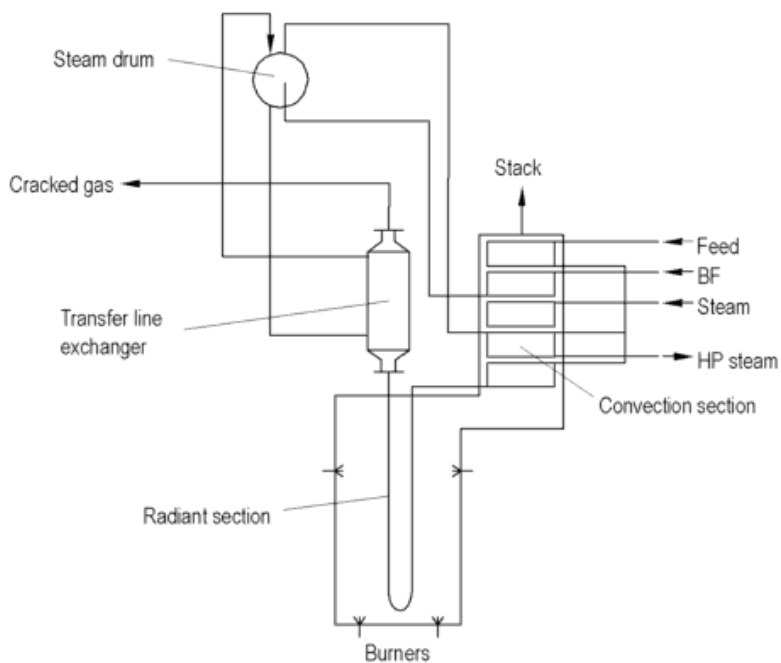
Figure 2 Schematic Diagram of an Industrial Process Furnace

2.2 Chemical Reaction of Ethane Cracking

The following indicate the typical chemical reaction of an ethylene cracking[18] and the energy activation, E with the kinetics constant, k:
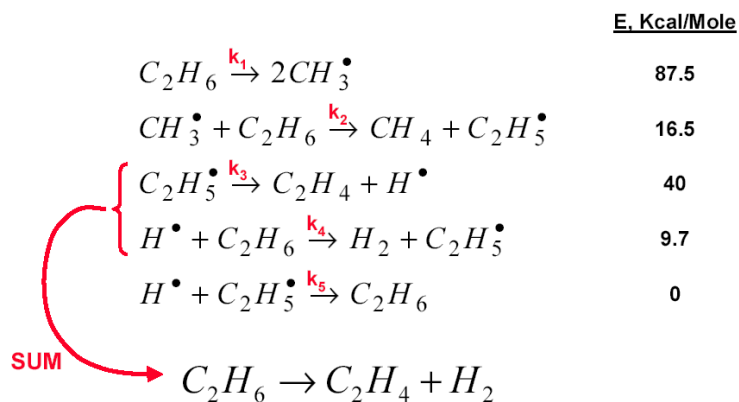
<div align="right">

E, Kcal/Mole

</div>

$$C_2H_6 \xrightarrow{k_1} 2CH_3^{\bullet} \qquad\qquad 87.5$$

$$CH_3^{\bullet} + C_2H_6 \xrightarrow{k_2} CH_4 + C_2H_5^{\bullet} \qquad\qquad 16.5$$

$$C_2H_5^{\bullet} \xrightarrow{k_3} C_2H_4 + H^{\bullet} \qquad\qquad 40$$

$$H^{\bullet} + C_2H_6 \xrightarrow{k_4} H_2 + C_2H_5^{\bullet} \qquad\qquad 9.7$$

$$H^{\bullet} + C_2H_5^{\bullet} \xrightarrow{k_5} C_2H_6 \qquad\qquad 0$$

SUM

$$C_2H_6 \rightarrow C_2H_4 + H_2$$

Figure 3 Ethane Cracking Reactions

Typically, the temperature requirement during the process for the conversion percentage is at 25%; 750°C, 50%; 775°C and 50-65%; 830°C.

5

2.3 Material Properties Tube Coil Alloy Steels

The material used for the Tube Coil inside the OPTIMAL furnace is Nickel-chromium steels[2]. Nickel steels are noted for their strength, ductility and toughness[17], while their hardness and resistance to wear characterize from the chromium steels.

Material Property	Value	Units
Modulus of Elasticity	2.2×10^{11}	Pa
Specific Gravity	8.4	Dimensionless
Density	8400	Kg/m^3
Melting Point	1400	^{o}C
Specific Heat	450	$Jkg^{-1}\,^{o}C^{-1}$
Thermal Conductivity	11.3	$Wm^{-1}\,^{o}C^{-1}$
Thermal Expansion	14×10^{-6}	$^{o}C^{-1}$

Table 1 Material Properties Nickel-Chromium Alloy Steels

Chromium Content (%)	Tensile Stress (MPa)	Elong. (%)
36	480	62
50	540-680	7-24
60	800-1000	1-2

Table 2 Tensile and Ductility Properties for Ni/Cr Alloy

Alloy Steels	Specific Resistance (Electrical Resistivity) mW-cm	Maximum Operating Temperature in air (^{o}C)
NiCr 80:20	108	1200
NiCr 70:30	118	1250
NiCr 60:15	112	1100
NiCr 40:20	105	1050
NiCr 30:20	104	1000

Table 3 NiCr Specific Resistance and Maximum Operating Temperature[19]

2.4 Model Equation

Due to the time averaging of the equations a closure model is required to account for turbulence, in addition to the total continuity, momentum and energy equations. In this work, the standard k–ε turbulence models applied. Omitting an explicit notation indicating that the variables are Reynolds-averaged[1], the resulting equations can be written as follows:

$$\sum_{j=1}^{3} \frac{\partial}{\partial x_j}(\rho u_j) = 0, \tag{1}$$

$$\sum_{j=1}^{3} \frac{\partial}{\partial x_j}(\rho u_i u_j)$$

$$= -\frac{\partial p_{\text{eff}}}{\partial x_i} + \sum_{j=1}^{3} \frac{\partial}{\partial x_j}\left((\mu + \mu_{\text{turb}})\right.$$

$$\times \left.\left(\frac{\partial u_i}{\partial x_j} + \frac{\partial u_j}{\partial x_i} - \delta_{ij}\sum_{k=1}^{3}\frac{2}{3}\frac{\partial u_k}{\partial x_k}\right)\right) + S_{Mi}, \tag{2}$$

$$\sum_{j=1}^{3} \frac{\partial}{\partial x_j}(\rho H_{\text{eff}} u_j) = \sum_{j=1}^{3} \frac{\partial}{\partial x_j}(\lambda + \lambda_{\text{turb}})\frac{\partial T}{\partial x_j} + S_E, \tag{3}$$

$$\sum_{j=1}^{3} \frac{\partial}{\partial x_j}(\rho u_j k) = \sum_{j=1}^{3} \frac{\partial}{\partial x_j}\left(\left(\mu + \frac{\mu_{\text{turb}}}{\sigma_k}\right)\frac{\partial k}{\partial x_j}\right)$$

$$+ P_k - \rho\varepsilon, \tag{4}$$

$$\sum_{j=1}^{3} \frac{\partial}{\partial x_j}(\rho u_j \varepsilon) = \sum_{j=1}^{3} \frac{\partial}{\partial x_j}\left(\left(\mu + \frac{\mu_{\text{turb}}}{\sigma_\varepsilon}\right)\frac{\partial \varepsilon}{\partial x_j}\right)$$

$$+ P_\varepsilon - C_{2\varepsilon}\rho\frac{\varepsilon^2}{k}. \tag{5}$$

Figure 4 Model Equation

The equations describe the conservation of mass (1), momentum (2), energy (3), turbulent kinetic energy k (4) and dissipation of turbulent kinetic energy ε (5). The left-hand sides of these equations contain the so-called convective terms, which also include the pressure term in the right-hand side of the momentum balance (2). The remainder of the right-hand sides contains the viscous

7

contributions and the source terms S. In the momentum equation (2) gravitation is included in the source term ($S_{Mx} = S_{My} = 0$ and $S_{Mz} = -\rho g$). The source term SE in the energy equation (3) includes the volumetric radiative heat release (Qrad, discussed in the next section). The source terms in the $k - \varepsilon$ equations are, respectively, defined as $S_k = P_k - \rho \varepsilon$ and $S_\varepsilon = P_\varepsilon - C_{2\varepsilon} \rho \varepsilon 2/k$. In the model simulation, the value for k and ε is set as default by the software, which is 0.9 and 1.22.

2.5 Heat Transfer inside Furnace Firebox

The major transfer of heat[11] in the furnace firebox is:

1. Radiation from the hot gas cloud to the final heat receiving surface

2. Heat re-radiated from hot refractory surface to the cold surface.

Even though most of the heat in the firebox is transfer by radiation, the combustion gases also transfer some convective heat to the surface of the tubes. The heat energy of the gasses passes away from the wall of the tube coil, resulting heat conduction into the ethane inside the tube coil.

2.6 API 573 – Inspection of Fire Boiler and Heaters

Based on the API 573[6], the metal temperature plays a major role in the type and severity of the deterioration of the heater tubes. The metal temperature of individual tubes or along the length of any specific tube coil of a given heater can vary considerably. The principal causes of abnormal variation in metal temperature are internal fouling of the tubes, which insulates the tube wall from the process and improper or poor firing conditions in the heater. Some potential signs of creep in tubes are:

a) Sagging caused by overheating or may also by improper spacing of hangers, uneven metal temperatures, or failure of one or more tube supports or hangers.

b) Bowing caused by uneven metal temperatures, which may be due to flame impingement or coke accumulation inside the tube. <u>Heating on one side of the tube causes greater thermal expansion on the hotter side and bowing toward the heat source.</u> Bowing may also be caused by binding of the tube in the tube sheets or improper suspension of the tube so that longitudinal expansion is restricted or by the use of improper tube lengths when individual tube replacement is made.

c) Bulging is generally an indication of overheating.

2.7 Three Dimensional Asymmetric Flow and Temperature Fields in Cracking Furnace

A three-dimensional flue gas flow fields and temperature profiles[9] are calculated (a same design used at OPTIMAL Furnace) which is 4/2/1 split design tube coil cracking furnace with long flame burners and an asymmetric flue gas outlet. The asymmetric flue gas flow fields are found to be compensated for by a net radiative heat transfer in the opposite direction, means that the temperature distribution in the furnace remains nearly symmetrical. Furthermore, a furnace simulation under conditions of non-uniform heating confirms the compensating nature of radiative heat streams in the furnace and resulted that non-uniform heating have improve the thermal efficiency of the furnace and the cracking results. (Please refer to Appendix 1 for more details in simulation results)

2.8 CFD Model

Computational Fluid Dynamic (CFD) in FLUENT[20] solver is base on finite volume method. Its work based on:

- Domain is discretized onto a finite set of control volumes (cells/meshing)

- General conservation (transport) equations for mass, momentum, energy, species, etc. are solved on this set of control volumes.

- Partial differential equations are descritized into a system of algebraic eruptions.

- All algebraic equations are then solved numerically to render the solution field.

The results will change with mesh refinement[4]. For example, a beam surface to examine stresses and it will increase with mesh that is more refined. This effect arises from two contributing factors. First, is that stresses are calculated based on displacement results, means that larger displacements lead to larger stresses. This contribution, however, is usually small. The second and more important factor is that smaller elements collect stress information closer to the surface where higher stresses reside. Therefore, the meshing[7] have to be planned to get an optimum result using GAMBIT software. Strategies for mesh optimization:

- All the mesh entities starting from the first and going to the last

- Only some entities selected ad-hoc (using a heap based on a relevant criterion, edge length if edges are to be processed, or using a quality threshold, etc.)

- All the entities, or only some of them, randomly picked.

2.9 Remark on Symmetry Conditions in Computational Homogenous Problem[3]

By using symmetry[3] approach, symmetry conditions to reduce computing times in problems involving finite element-based multi-scale constitutive models of non-linear heterogeneous media. Two types of symmetry often present in practical interest have been considered: staggered-translational and point symmetry.
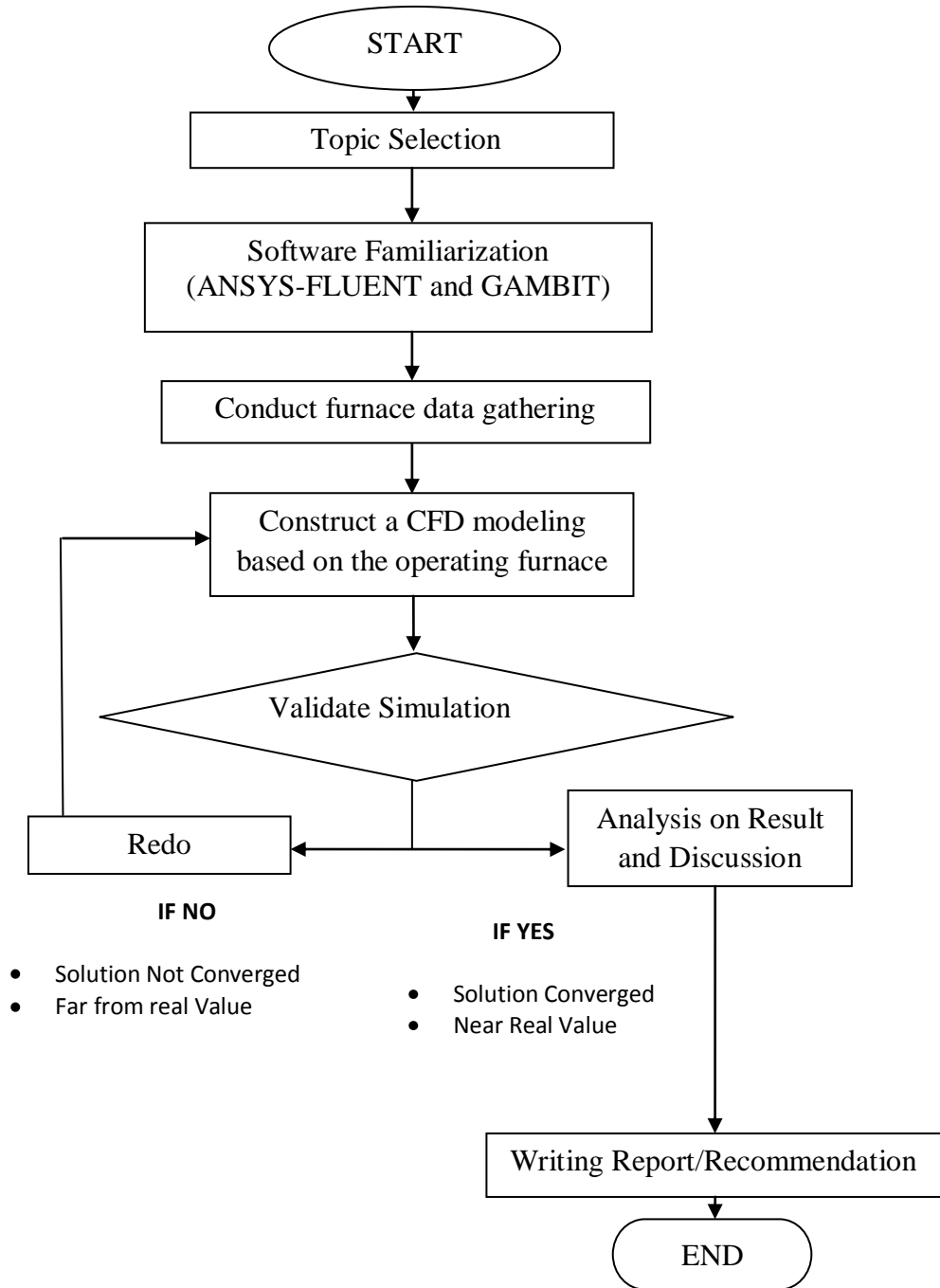
2.10 Grid Independence

The grid independence[16] achieved via successive levels of grid refinement. Results obtained from grid dependent solutions may prove to be costly and time consuming that is we have to do grid independence.

CHAPTER 3

METHODOLOGY

3.1 Execution Chart

START

Topic Selection

Software Familiarization
(ANSYS-FLUENT and GAMBIT)

Conduct furnace data gathering

Construct a CFD modeling
based on the operating furnace

Validate Simulation

Redo

Analysis on Result
and Discussion

IF NO

IF YES

- Solution Not Converged
- Far from real Value

- Solution Converged
- Near Real Value

Writing Report/Recommendation

END

3.2 Milestone and Project Planning

Item	February				March				April				Mei				June				July			
	1	2	3	4	1	2	3	4	1	2	3	4	1	2	3	4	1	2	3	4	1	2	3	4
Research and Study	■	■	■	■	■	■	■	■																
Preliminary Research Work	■	■	■	■																				
Submission of Prelim Report			▲																					
ANSYS Familiarization																								
Identification										■	■													
Tutorials											■	■												
Submission of Progress report										▲														
Seminar Presentation										▲														
3D Modelling																								
Furnace Modelling																	■	■						
Submission of Interim Report																			▲					
Oral Presentation																			▲					

Table 4: Project Planning and Milestone FYP1

Item	July				August				Septem				October				Novemb			
	1	2	3	4	1	2	3	4	1	2	3	4	1	2	3	4	1	2	3	4
ANSYS-Fluent and Gambit	■	■	■	■	■	■	■	■	■	■	■	■								
Seminar											▲									
Data Collection														▲						
Analysis Result													■	■	■	■				
Comparison													■	■						
Poster Exhibition														▲						
Oral Presentation																		▲		
Submission of Dissertation																		▲		

Table 5: Project Planning and Milestone FYP2

Important Dates:

Seminar:	28th September 2010
Poster Submission:	11th October 2010
Data Collection:	24th October 2010
Dissertation Draft:	1st November 2010
Oral Presentation:	11th November 2010
Hardbound Dissertation:	7 days after oral presentation

13

3.3 Temperature Data Gathering

The data taken will be comparing to the data obtained from the simulation of the furnace. The temperature data gathering is taken from the following peephole at the furnace wall (1/8 of full Furnace Firebox) by using pyrometer:
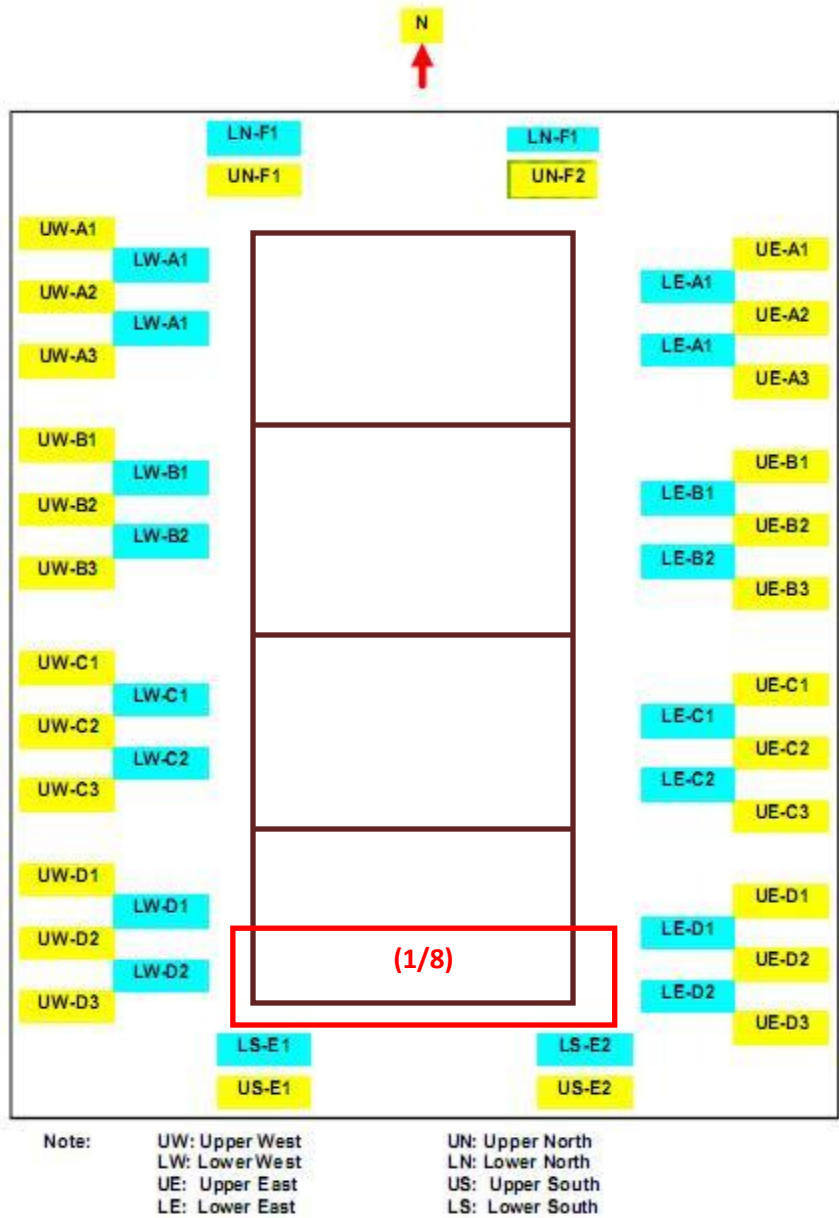

Figure 5 Peep Hole for Temperature Data Gathering

Figure 6 Infrared Pyrometer used by Furnace Operator from OPTIMAL Chemicals (M) Sdn. Bhd to take data in the firebox.

3.4 Furnace Modeling and Simulation

The following are modeling and meshing by using GAMBIT software. After done the modeling and meshing, it is export into Fluent software for simulation.

Wall Burner 2

Wall Burner 1

Floor Burner
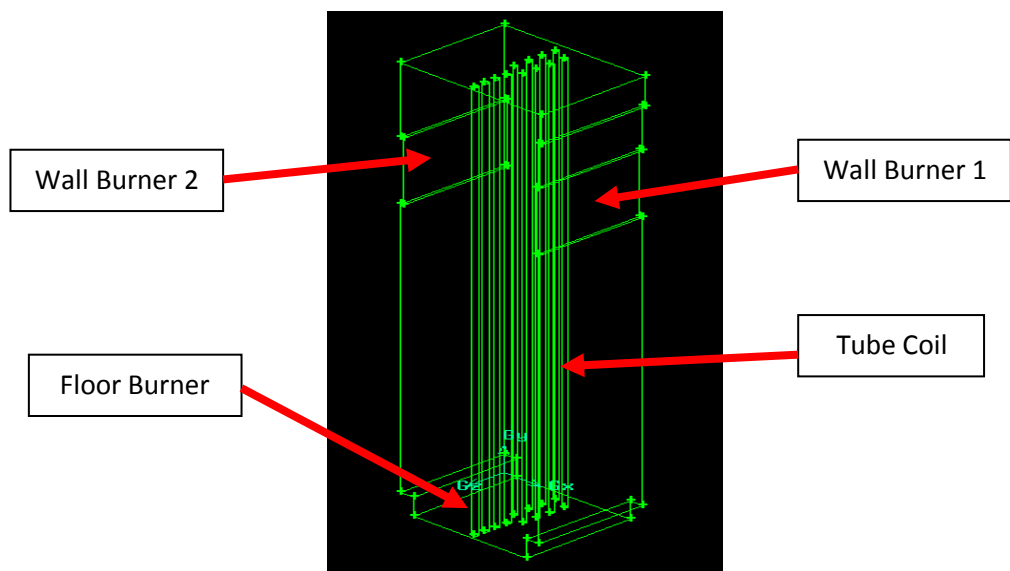
Tube Coil

Figure 7 Furnace (1/8) 3D Models in Gambit
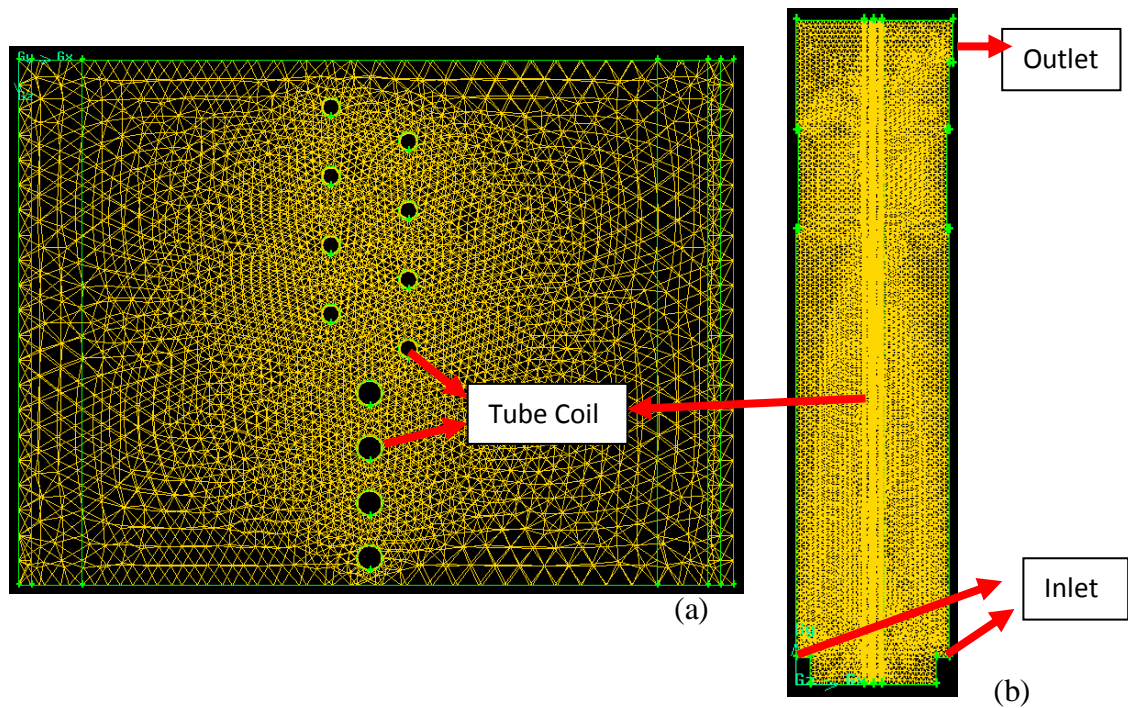
Figure 8: Mesh by using Tetrahedral/Hybrid with size function attach to tube coil face (a) Top View (b) Side View

Summarizing Mesh on Firebox Furnace:

Total Nodes: 174496

Total Elements: 886435

Type: Tetrahedral/Hybrid with 0.1 Interval Size Spacing

Size Function:

Start Size- 0.032

Growth Rate- 1.12

Maximum Size- 0.2

3.5 Calculation

The following calculation is needed for the meshing and simulation.

Size Function (SF):

$$\Delta Xn = \Delta Xo * (SF)^n$$; Where Xn is the size limit, Xo is the start size and n is the number of meshes.

By Setting:

$\Delta Xn = 0.05$ m

$\Delta Xo = 0.016$ m

$n = 200$

We get the mesh Size Function (SF) = **1.0586**

Mass Flow rate, m: ρ x A x V;

where ρ is density, A is cross section area and V is velocity.

By Setting,

P= air density= 1.225 kg/m3

A= cross section area= (0.25 x 2.75) = 0.6875

V= velocity inlet= 0.01m/s (from plant operation)

m= 1.225 x 0.6875x 0.01= **0.00843 kg/s**

Hydraulic Diameter, Dh:

$$D_H = \frac{4A}{P}$$

Where A= Cross Sectional Area and P= Perimeter of the cross section.

A= Length X Height = (0.25 x 2.75) = 0.6875

P= 2Length +2 height = (2x2.75 +2x0.25) = 6

Thus, Dh= 4(0.6875)/6 = **0.46 m**

3.6 Boundary Conditions Setting

Following are the value for Boundary Conditions:

1- Materials: Air (with default value)

2- Inlet: Velocity Magnitude: 0.01 m/s

Hydraulic Diameter: 0.46 m

3- Outlet: Gauge Pressure: -60 MPa

Target Mass Flow: 0.00843 kg/s

Hydraulic Diameter: 1.1 m

4- Wall Burner 1: Temperature: 1270K

5- Wall Burner 2: Temperature: 1321K

6- Floor Burner: Temperature: 1360K

CHAPTER 4

RESULTS & DISCUSSION

4.1 Furnace Data at Normal Operation (Ethane Cracking)

Please refer to Appendix 1.

4.2 Furnace Full Dimension (Firebox)

Height:
12.01 m

Length:
16.45 m

Width:
2.750 m
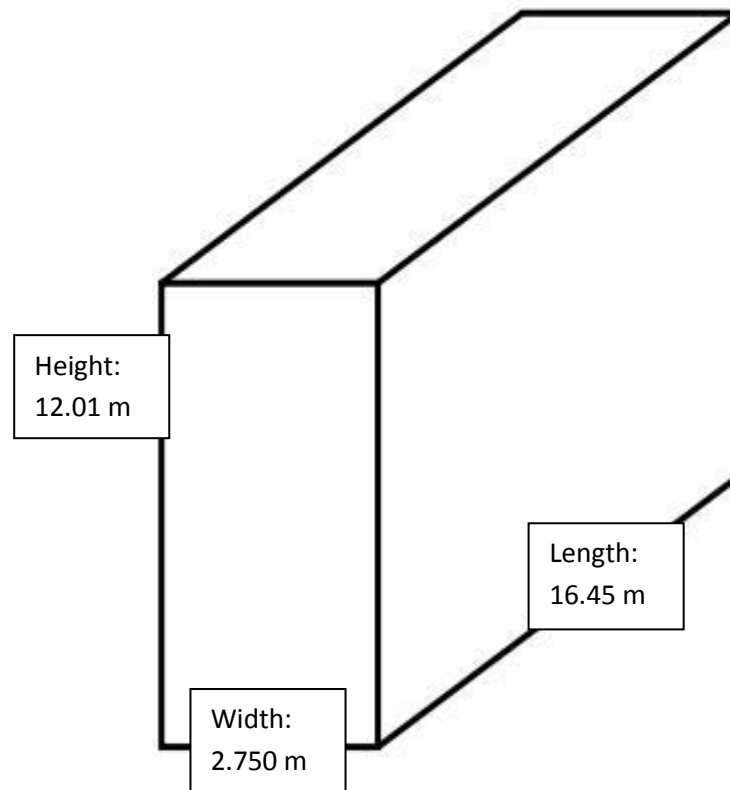
Figure 9 Furnace Full Dimensions

4.3 Simulation Results in Fluent Software

The first simulation was to assume the flow is in steady state. The boundary condition of the model was set to the surface wall temperature of the firebox, which are up to 1260 Kelvin at the wall burner 1 and 1310 Kelvin at wall burner 2, while the floor burner is 1360 Kelvin. However, the simulation still does not converge into solution after reaching 8000 iterations.
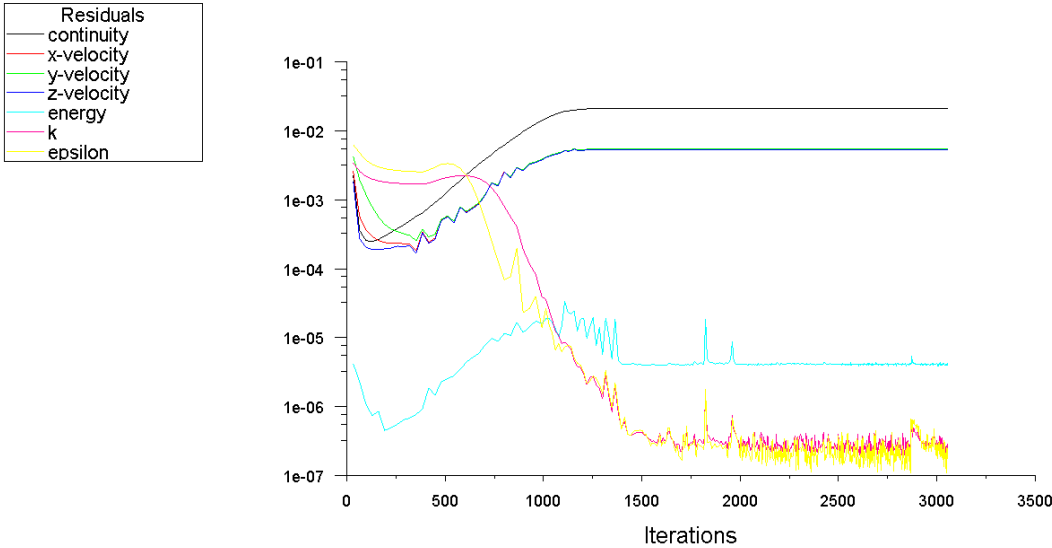
Figure 10 Steady-State Iteration (3000)
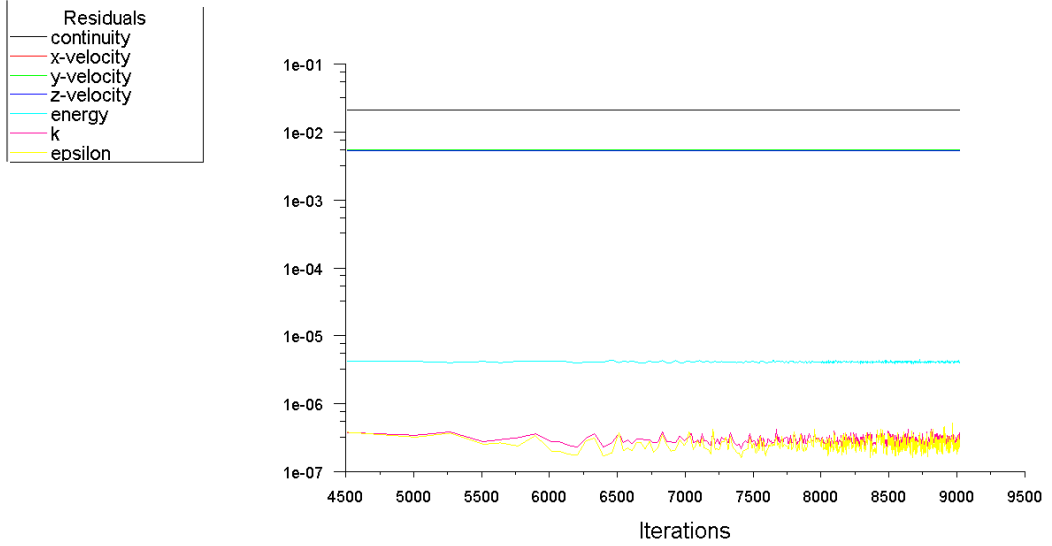
Figure 11 Steady-State Iteration (Continued up to 9000)

20

During the iterations, the flow mass rate at the inlet and outlet were also been monitor to see the simulation has reached the convergence solution. The result obtained shows that the mass flow inlet and mass flow outlet are approximately the same, which lead us to an indication of the solution has converge.

Mass Flow Rate	(Kg/s)
Inlet	0.012599121
Outlet	-0.012584727
Net	1.439359×10^{-5}

Table 6 Mass Flow Rate Convergence

The result of temperature distribution obtained from the steady-state condition as follows:
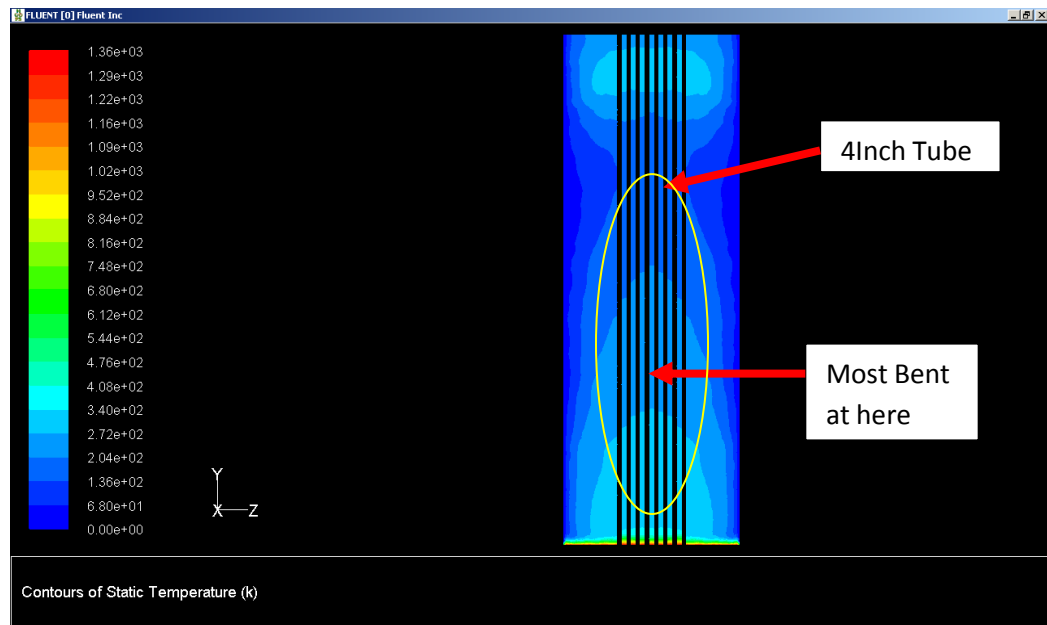
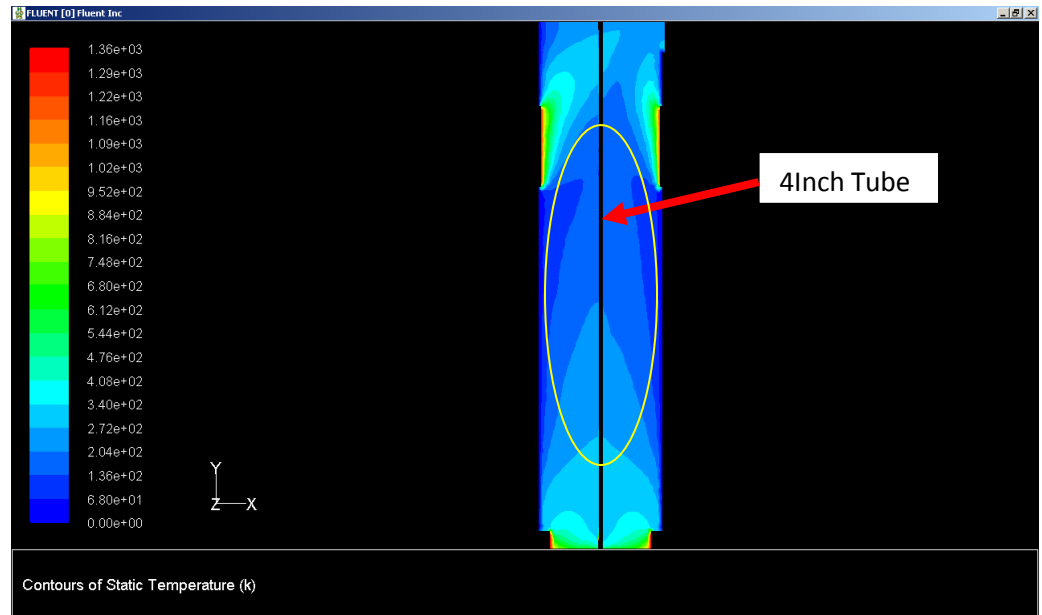**Figure 12 Heat Distributions from Side View (at the middle)**

Figure 13 Heat Distributions from Front View

This clearly shows that the heat distribution is concentrated towards the 4-inch tube coil at the middle of the system (in the yellow circle). That means the heat are more being conduct near the 4-inch Tube Coil (black color in the image).

Although the wall burners have slightly difference between both walls, the temperature distribution has no affect but the floor burner contribute most of the temperature distribution from bottom to the top.

From the Residual Monitoring result of the first simulation, we can assume the flow is an unsteady-state because of the fluctuation of the graph and non-convergence. Therefore, the second simulation is set into the unsteady-state flow with Time Step Size, Δt is 0.05s by using Fixed Method. Following are the results that have been observe:
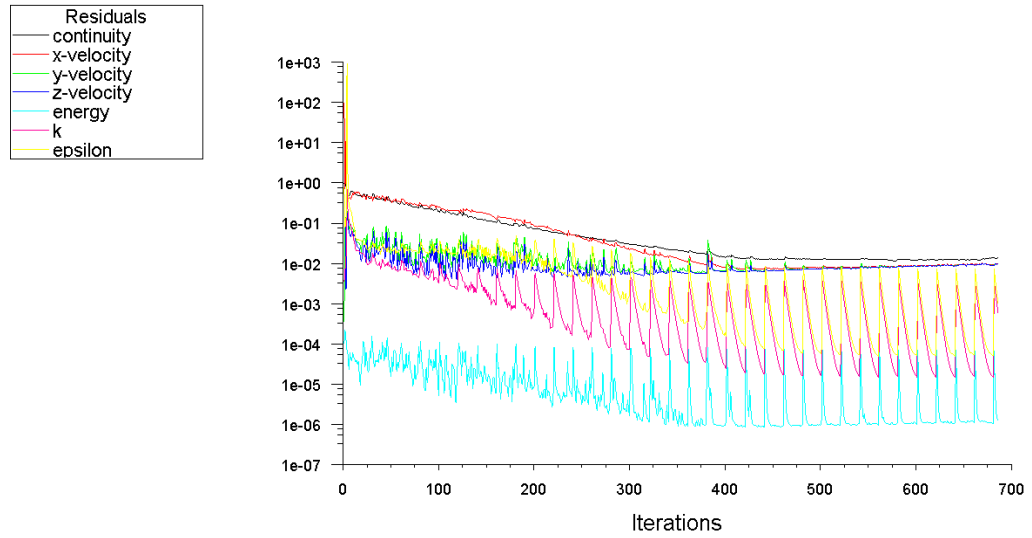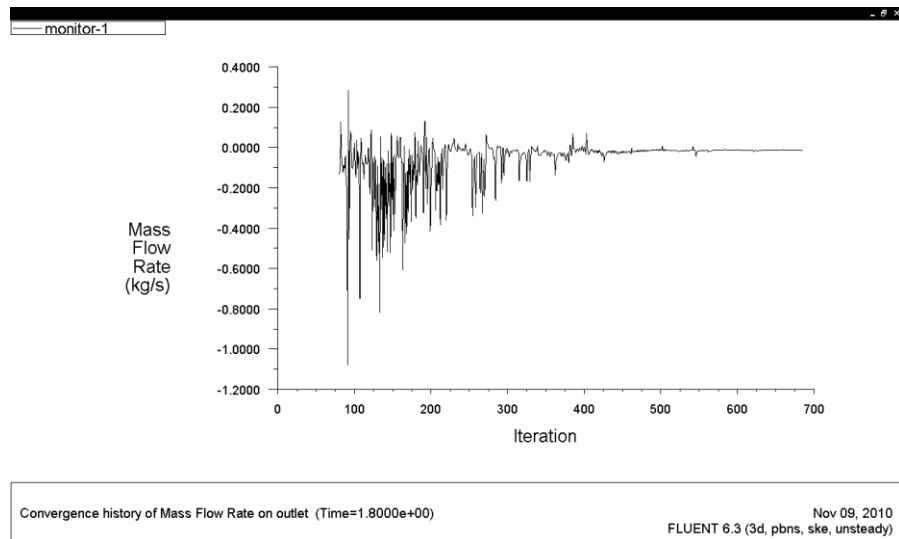
Figure 14 Residuals Unsteady-State

Figure 15 Mass Flow Rate Unsteady-State

Due to time constraint, the second simulation by using unsteady-state condition will be consider as a way forward for this project.

4.4 Temperature Data Gathering from Plant Operation

The Temperature data is taken at a specified location on the 4-Inch tube coil surface inside the furnace firebox, which is at the height of 6.4 meter from bottom, 1.9 meter from the front, and 1.25 meter from the sidewall. The temperature at the location is 1186 Kelvin. Please refer Table 4 in Appendix 2 for more details on temperature data gathering.

4.5 Error Analysis

The error analysis is calculated to determine the difference between the real time operation and the simulation by the computer. A point at inside the furnace firebox (please refer to Appendix 2 for detail) that has taken is to be compare with the same point location in the simulation to get the error percentage. The percentage error calculation:

(Temperature in firebox)- (Temperature in simulation)

---   X   100%

(Temperature in Firebox)

At the height of y= 6.4m from the bottom in the Fluent plot temperature graph; the x and z value has been taken.
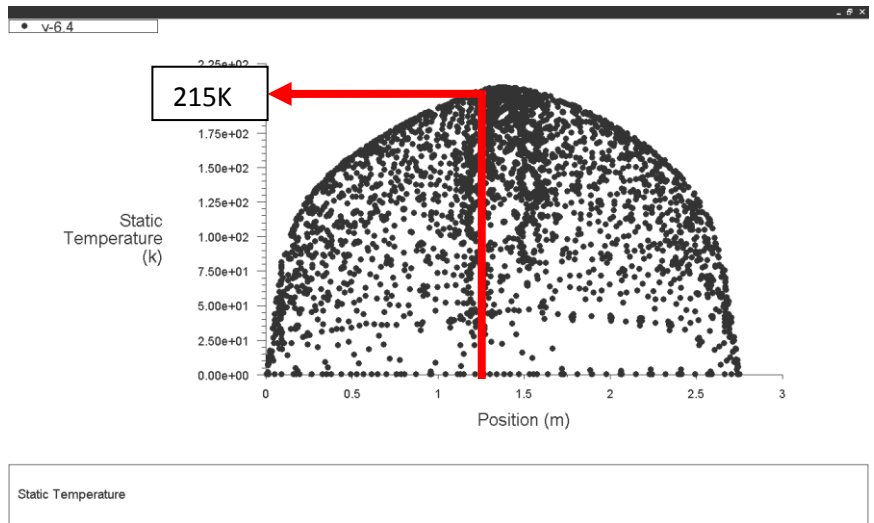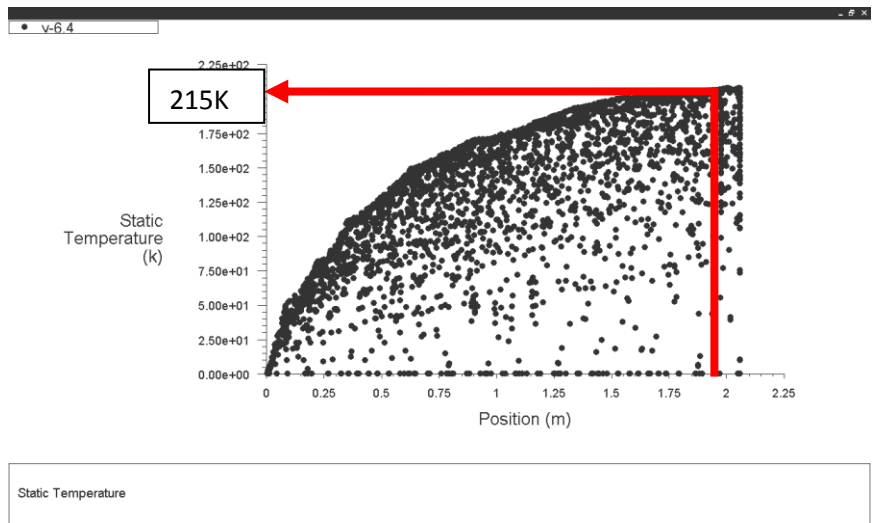
Figure 16 Plot X-Y Graph

Figure 17 Plot Z-Y Graph

From the above plot graph, the temperature at a height y= 6.4 m, x= 1.25m, and z=1.9m, is 215Kelvin. However, at the same location inside the firebox taken data by Infrared pyrometer, the temperature is at 1186 Kelvin.

25

Therefore, the error percentage is:

$$= \frac{215\text{-}1186}{215} \quad x \quad 100\%$$

$$= \quad \text{-452 \% (negative; smaller than the real value)}$$

The error obtained is too high for the temperature comparison between simulation and the real value because of the assumption made only consider heat transfer from the wall burner and floor burner in the simulation. Besides that, the temperature taken at the Plant may vary because of the equipment used for collect the data.

CHAPTER 5
CONCLUSIONS & RECOMMENDATIONS

5.1 Conclusions

As a conclusion, the heat distribution inside the furnace firebox is uniformly distributed from the bottom to the top of the firebox. The slight difference between the wall burners temperature at both sides has no effect to the bottom part of the firebox (where the bending occurs). However, the heat distribution is more concentrated at the 4-Inch tube coil in the middle of the coil system. This can be related to the phenomena of most bending coil occurred at the 4-Inch tube coil (Please refer to Appendix 3 for detail location of the bending tube coil inside Furnace Firebox). Therefore, for the future design of the coil system, it is suggest to use a higher strength material (Such as Ni/Cr with 70/30) for the 4-Inch tube coil than the 3-Inch tube coil material strength (Ni/Cr with 80/20).

In addition, based on the simulation, the heat is accumulated most near the top and the bottom of the furnace firebox. This will extend the tube coil by thermal expansion at both ends towards the same direction, and then the tube will bend at the point where the weak point of the tube coil. This thermal expansion also explained the counter weight system movement at the firebox (Please refer to Appendix 3). The free spaces at the bottom of the tube coil need always to be clear for the tube coil to expand.

By completing this project, the heat distribution can be confirm as one of the factor contribute to the failure of tube coil bending inside the furnace firebox.

4.2 Recommendations

An improvement to the simulation is highly recommended to achieve the value near the real value in the furnace firebox. For example, to take into consideration the other sources of heat transfer such as radiation from the refractory wall and convection from the combustion air. The air density also needs to be specify with the exhaust combustion in the firebox.

Besides, the equipment for collecting temperature data, a thermal camera is recommend to use for taking the temperature readings in the furnace firebox instead of using infrared pyrometer.

Furthermore, this project should continue the simulation in an unsteady-state flow condition to achieve a better result. In addition, the meshing should be examined first to achieve the grid independence before exporting the model into Fluent software for simulation.

REFERENCES

1. A. J. M. Oprins, G. J. Heynderickx (2002), Calculation of three-dimensional flow and pressure fields in cracking furnaces.

2. Azom.com. (2001, September). Retrieved March 2010, from Nickel Chrome Alloys: http://www.azom.com/details.asp?ArticleID=916

3. Flores, S., & Neto, S. (n.d.). Remarks on Symmetry Conditions in Computational Homogenisation Problems.

4. Frey, P. J., & George, P. L. (2000). *Mesh Generation.* Oxford: HERMES Science Europe Ltd.

5. Incropera, Dewitt, Bergman, & Lavine. (2007). *Introduction to Heat Transfer.* Asia: John Wiley & Sons.

6. Inspection of Fired Boiler and Heaters Recomended Practice 573. (2003, February). *American Petroleum Institute (API)* , pp. 15-18.

7. Kurowski, P. M. (2004, November 4). *A closer look at Model Meshing*. Retrieved March 2010, from Machine Design: http://machinedesign.com/article/a-closer-look-at-model-meshing-1104

8. Moaveni, S. (2008). *Finite Element Analysis Theory And Application Third Edition.* New Jersey: Pearson Prentice Hall.

9. Oprins, A. J., Heynderickx, G. J., & Guy, M. B. (2001). Three-Dimensional Asymmetric Flow and Temperature Fields in Cracking Furnaces. *Ind. Eng. Chem. Res.* , 1-8.

10. *ProcessModeling.org*. (n.d.). Retrieved March 2010, from Three-Dimensional Model of System Furnace- Heated Body: http://www.processmodeling.org/furnace/model3d/furnace%20modeling%203d.html

11. Rosaler, R. (2002). *Standard Handbook of Plant Engineering 3rd Edition.* McGraw-Hill.

12. T. S., Nakasone, Y., & S. Y. (2006). *Engineering Analysis Software.* Burlington: Elsevier Butterworth-Heinemann.

13. Wikipedia, t. f. (n.d.). *Cracking (chemistry)*. Retrieved from http://en.wikipedia.org/wiki/Cracking_%28chemistry%29

14. Wikipedia, t. f. (n.d.). *Furnace*. Retrieved from http://en.wikipedia.org/wiki/Furnace

15. Y. A., & M. A. (2007). *Thermodynamics An Engineering Approach Sixth Edition (SI Units)*. Singapore: McGraw-Hill Higher Education.

16. Ronald J.Chila, Deborah A.Kaminski(2006). *Automated Grid Independence Via Unstructured Adaptive Refinement*. Fluid Dynamic Conference. San Francisco, California.

17. Material Properties Nickel-Chromium. *http://www.heating-element-alloy.com/nickel_chrome_alloys.html*.

18. *Thermal Cracking of ethane mixture.* Gilbert F Formet.Paul S Van Damme. Kinetics Technology International. The Hague, The Netherlands.

19. *Wear Resistance and Maximum operating Temperature NiCr* http://www.heating-element-alloy.com/nickel_chrome_alloys.html

20. *Introductory ANSYS- FLUENT Notes* December 2006. http://www.fluentusers.com

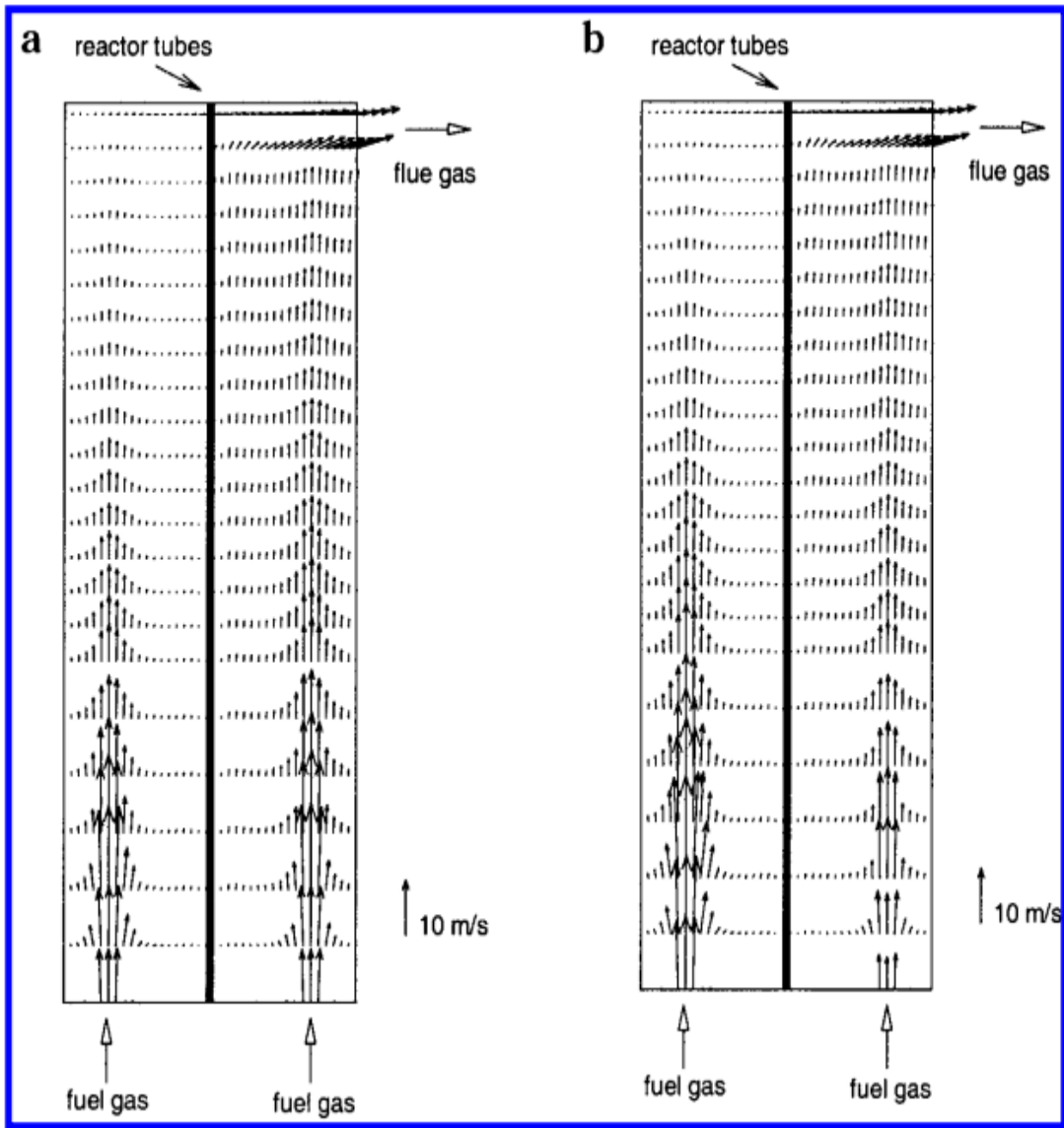**APPENDICES**

APPENDIX 1 (Literature Review)

Figure 18 Flue Gas Velocity Vertical Cross Section (a) Uniform Heating (b) Non-Uniform Heating
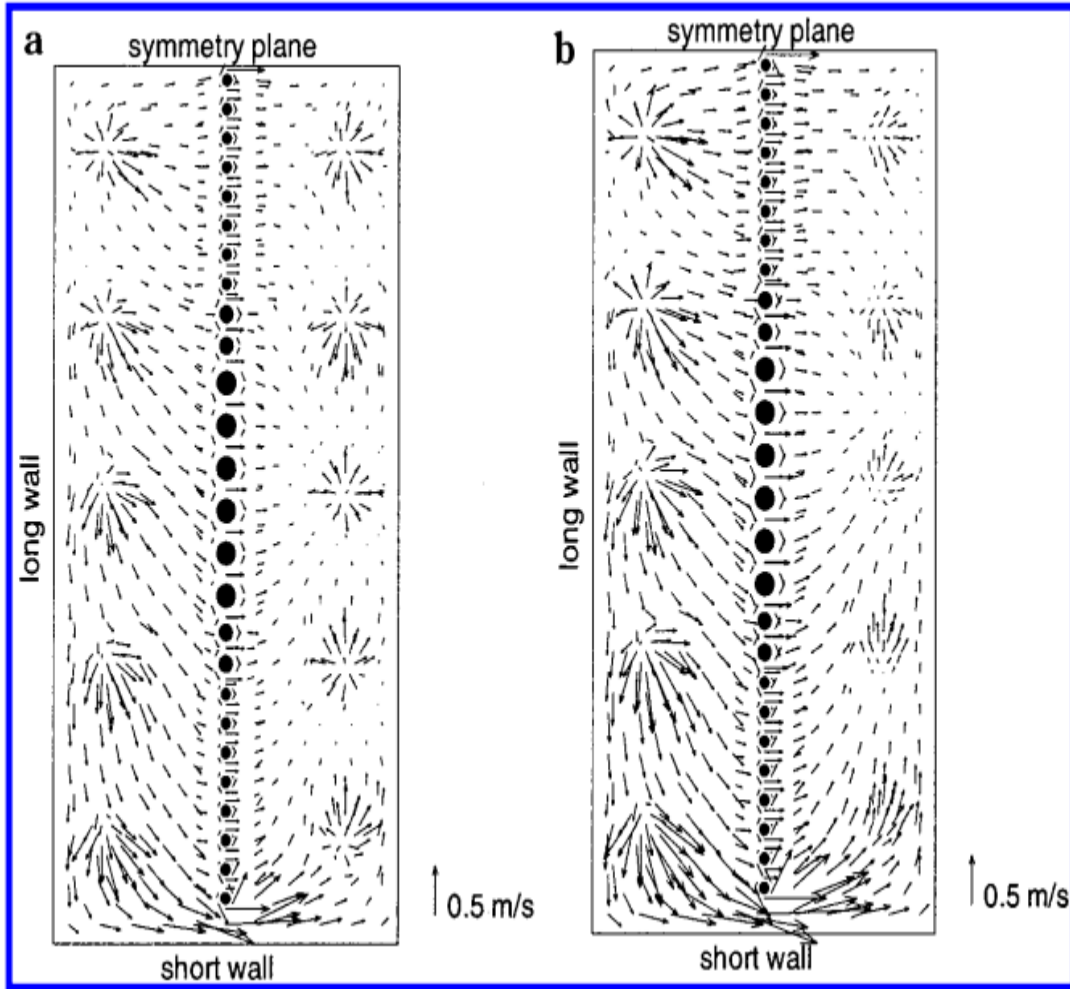
Figure 19 Flue Gas Velocity Horizontal Coss Section (a) Uniform Heating (b) Non-Uniform Heating

Results	Case 1 (Uniform Heating)	Case 2 (Non-Uniform heating)
Flue Gas Outlet Temperature	1442	1427
Furnace Efficiency (%)	45.4	46.1
Maximum Heat Flux (kW/m^2)	132	131
Coil Outlet Temperature (K)	1108	1114
Flue gas outlet Velocity (m/s)	7	7
Max Flame Temperature (K)	2100	2100
Max Flue Gas Velocity(m/s)	16	20

Table 4 Simulation Results

APPENDIX 2 (Data Gathering)
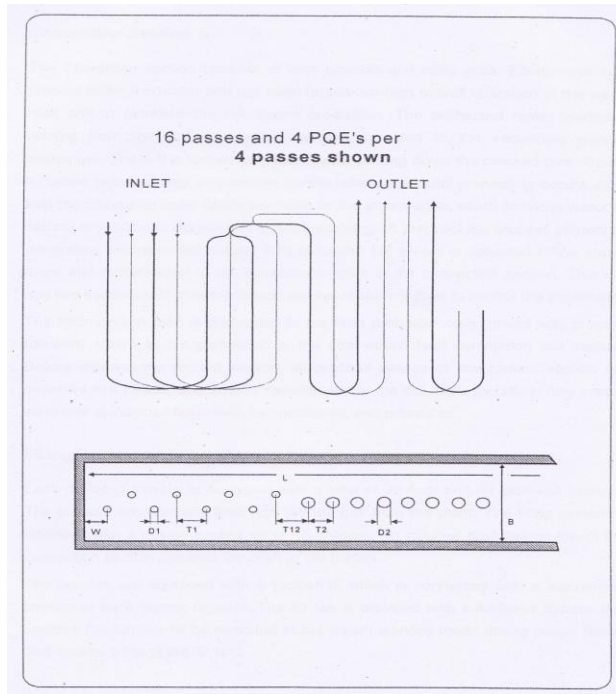
Figure 20 Tube Coil Section (4/2/1 Split Coil)

Wall Burner 1	Wall Burner 2	Floor Burner	At Height: 6.4m
1040	991	1076	835
1002	1014	1059	849
1039	990	1080	907
1005	1015	1060	862
1042	1001	1082	901
1110	1009	1058	890
1021	1012	1095	891
1048	966	1053	823
1073	957	1098	899
1032	980	1052	877
1048	1000	1099	912
1092	948	1054	866
1130	976	1078	872
1204	1021	1080	889
1078	999	1097	891
1039	987	1092	899
1032	982	1083	884
1023	986	1038	871
1083	992	1092	857
1038	1007	1082	897
1022	1028	1034	910
1037	1004	1103	861
1034	998	1067	880
1025	976	1078	849
1040	983	1080	847
1035	1009	1059	898
Average: 1048	997	1087	913

*Note: All data taken in Degree Celcius with an interval of 10 second

Table 8 Temperature Data Gathering (Degree Celsius)

At Height 6.4 meter from bottom, 1.9 meter from the front, 1.25 meter from the side wall.
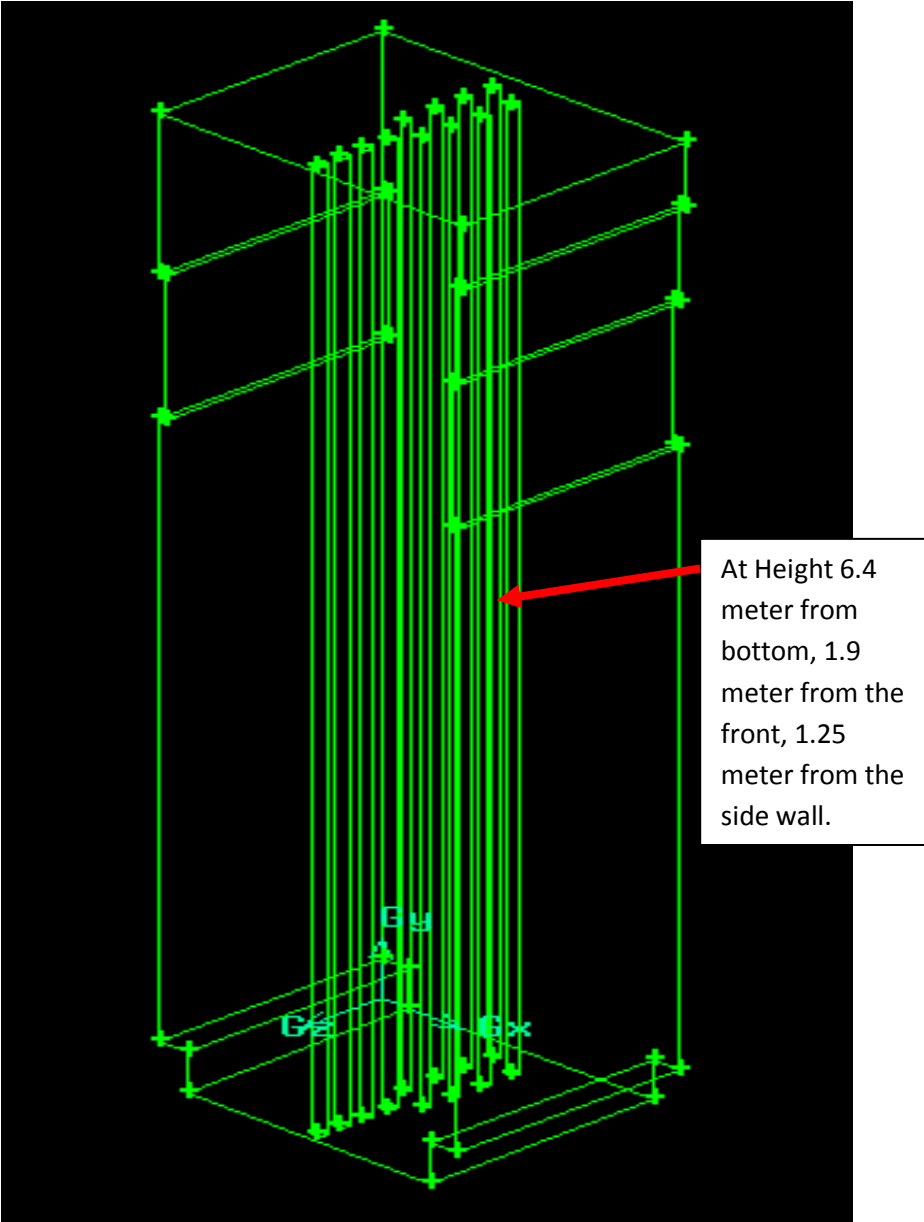
Figure 21 Temperature Point Location For Comparison

The following are the previous thermal imaging for inspection inside furnace firebox 1 obtained from OPTIMAL outsourcing to SIRIM Berhad in the year 2008:
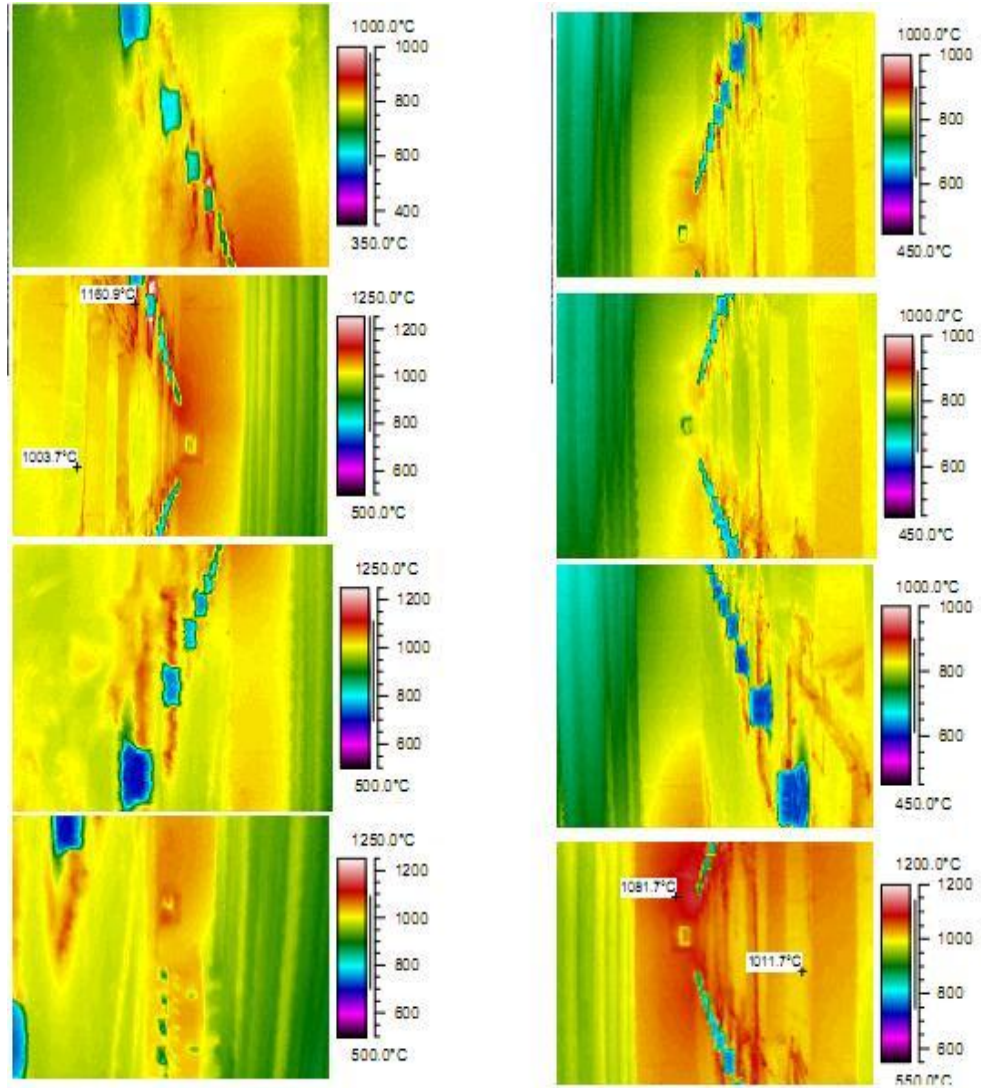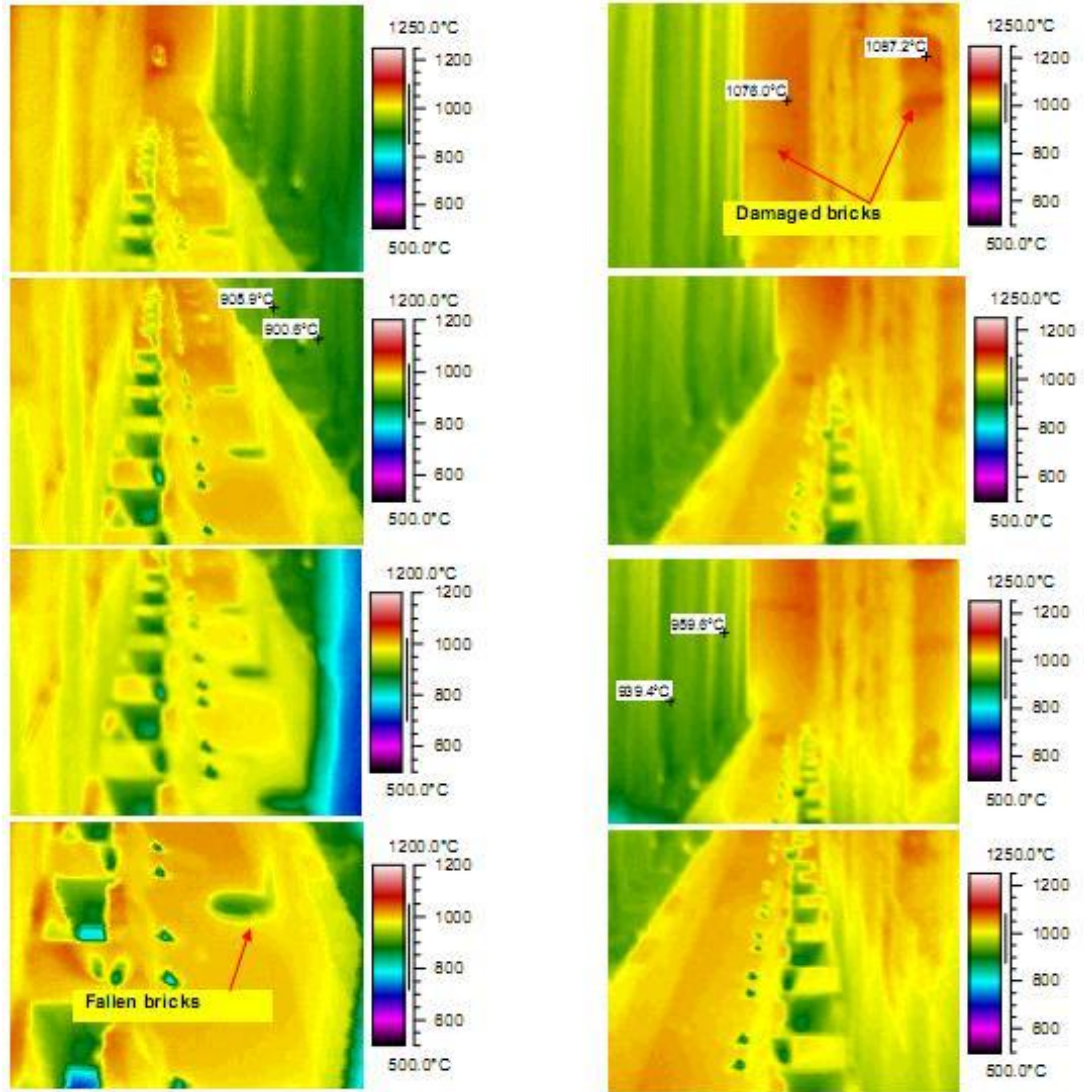

Figure 22 Sidewall Burner Thermography

Figure 23 Floor Burner Thermography

Flue Gas

		CASE 1	CASE 2
Flue gas temperature at cross over	TI-1301-53A/B	1185	1166 °C
Furnace draft at cross over	PC-1301-52C	-0.59	-0.59 mbar g
Flue gas temperature HTC II outlet	TI-1301-33/34	976.2	953.4 °C
Flue gas temperature HHP-steam superheater II outlet	TI-1301-31/32	829.9	806.9 °C
Flue gas temperature HHP-steam superheater I outlet	TI-1301-29/30	652.8	631.5 °C
Flue gas temperature HTC I outlet	TI-1301-23/24	429.4	412.2 °C
Flue gas temperature BFW ECO II outlet	TI-1301-21/22	289.9	284.0 °C
Flue gas temperature BFW ECO I outlet	TI-1301-19/20	200.1	194.9 °C
Flue gas temperature feed preheater outlet	TI-1301-17/18	144.9	140.4 °C
Oxygen content in flue gas	AC-1361-04A	2	2 Vol%
Carbonmonoxid content in flue gas	AI-1361-04B	<1	<1 Vol-ppm

Fuel Gas

		CASE 1	CASE 2
Fuel gas pressure in fuel / pilot gas header	PC-1301-157/158	4.5	4.5 bara
Heat duty per furnace half	QC-1301-72/73	31.24	29.24- MW
Heat duty ratio floor/side wall burners coil system A&B	QFC-1301-70/71	60:40	60:40

Figure 24 Normal Operations (Ethane Cracking)

Figure 25 Furnace Process Operation OPTIMAL Chemicals Computer System

APPENDIX 3 (Industrial Training)
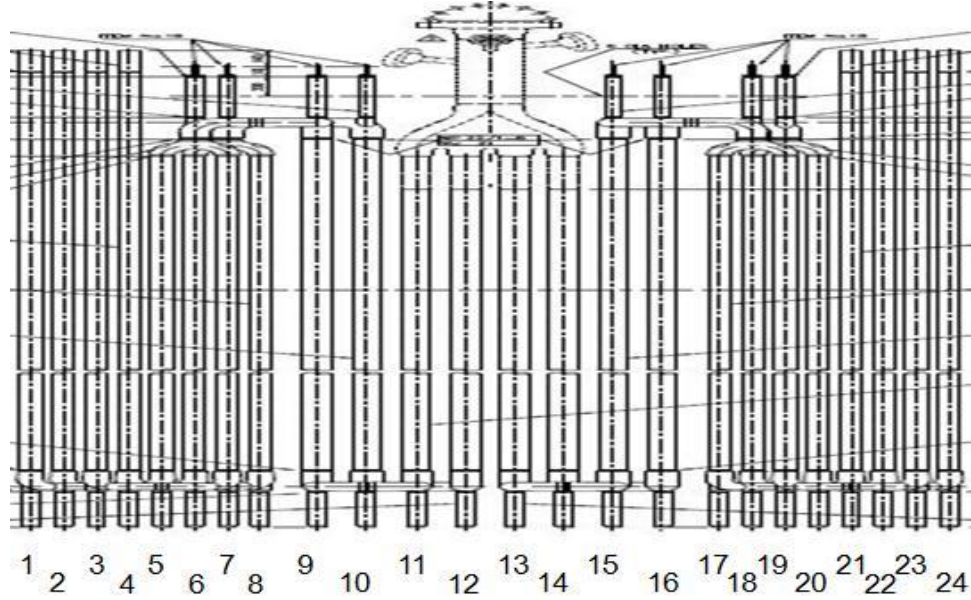
Bending Result

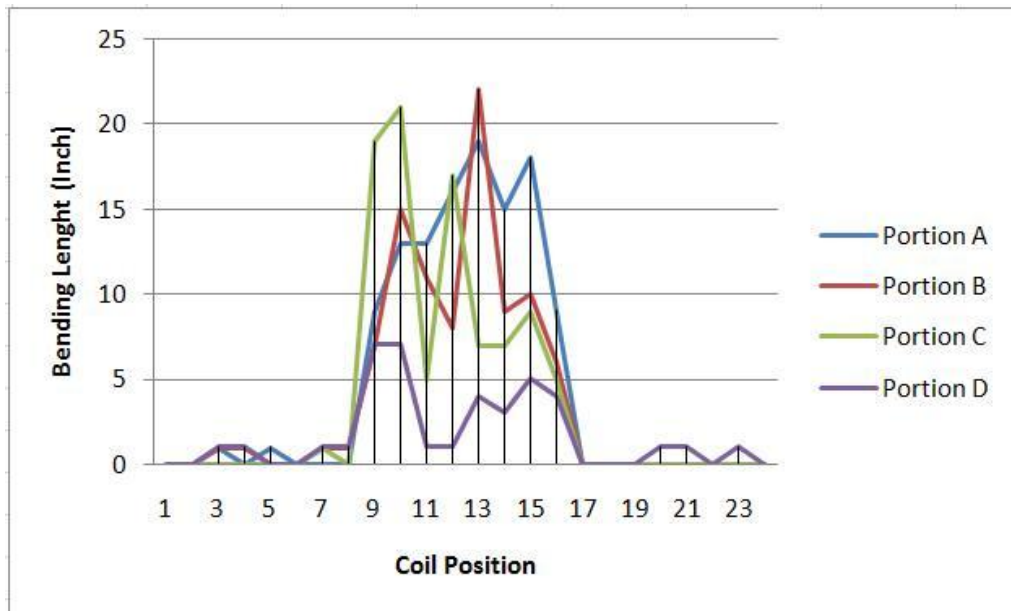**Figure 26 A Portion of Tube Coil Position**

Figure 27 Tube Coil Bending Position

- After tubing alignment and not operating on 15/11/09

Figure 28

- After start up and operating on 25/11/09

Focus on this black hole

Figure 29

As we see at the black hole indicator of the counterweight between the operating dates, we found that the counterweight move upward for about 8-10 Inch during the hot condition. Next page are the schematic explained on this matter:
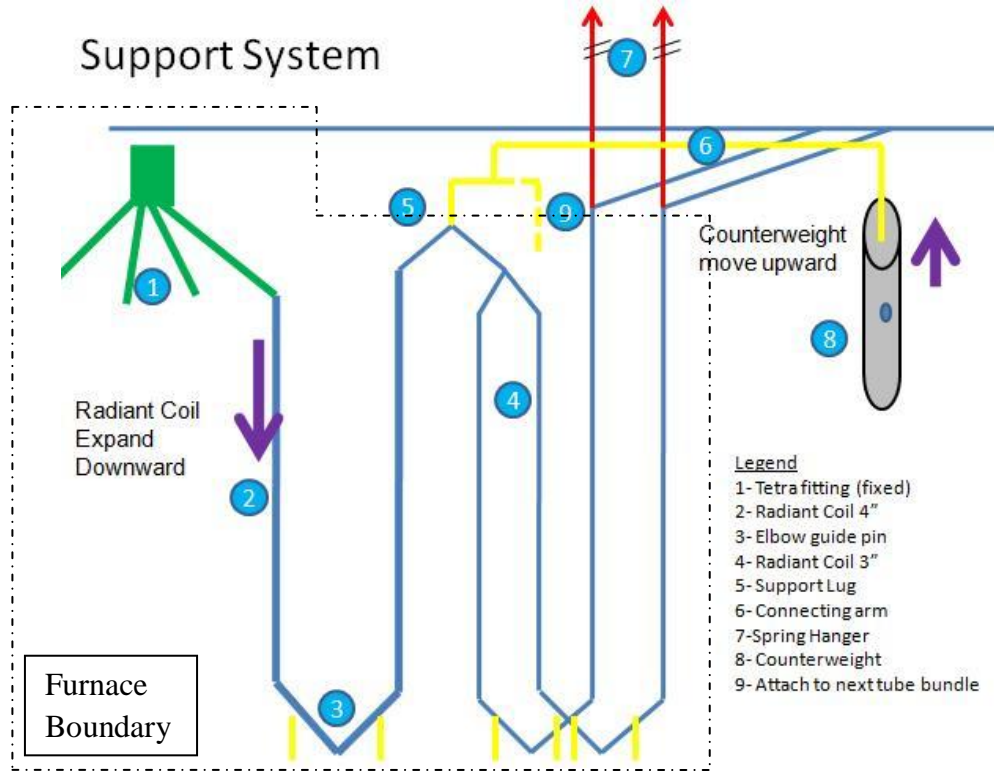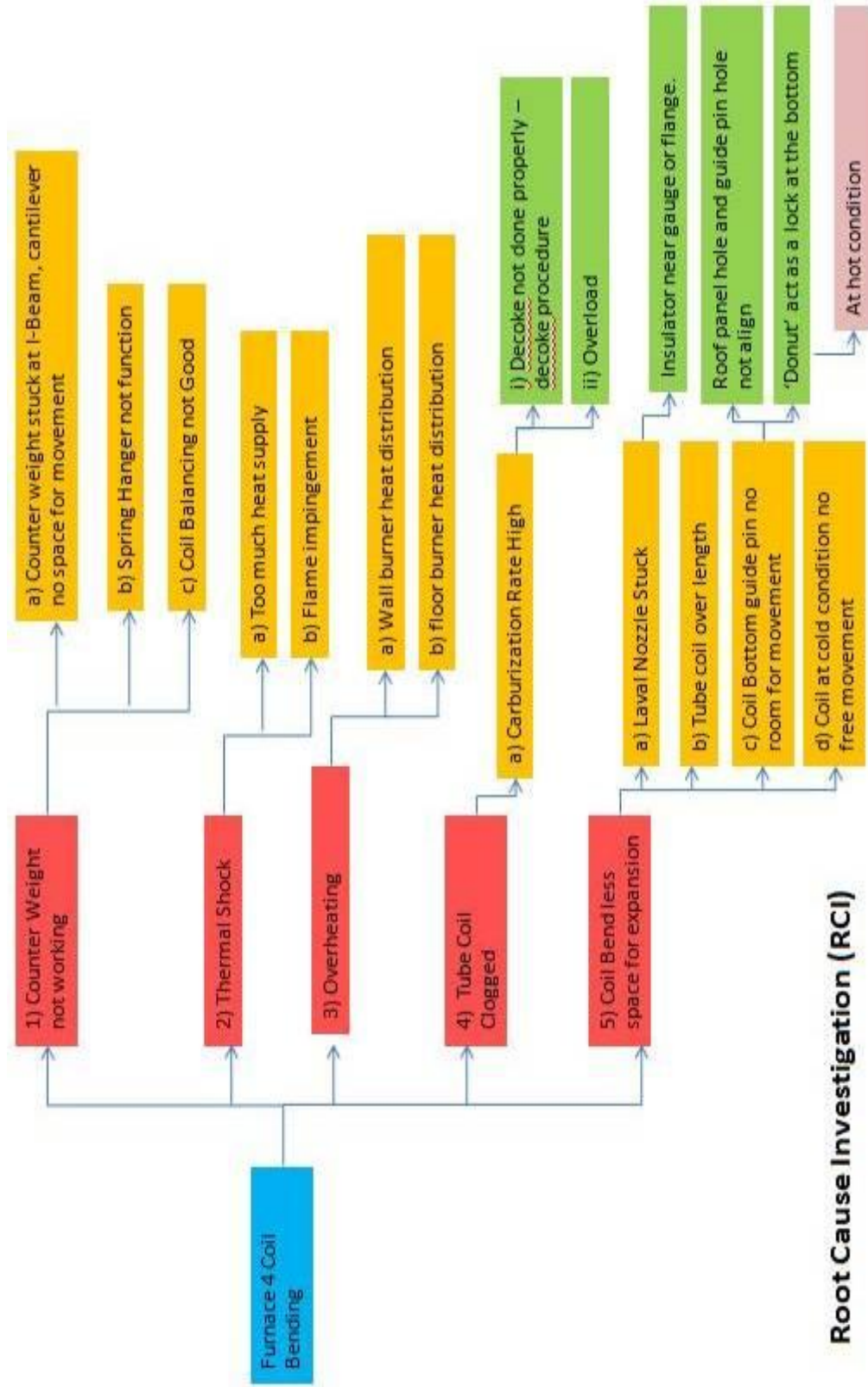
Figure 27 Support System

Figure 28 Root Cause Investigation

Root Cause Investigation (RCI)

Furnace 4 Coil Bending

1) Counter Weight not working
- a) Counter weight stuck at I-Beam, cantilever no space for movement
- b) Spring Hanger not function
- c) Coil Balancing not Good

2) Thermal Shock
- a) Too much heat supply
- b) Flame impingement

3) Overheating
- a) Wall burner heat distribution
- b) floor burner heat distribution

4) Tube Coil Clogged
- a) Carburization Rate High
  - i) Decoke not done properly – decoke procedure
  - ii) Overload

5) Coil Bend less space for expansion
- a) Laval Nozzle Stuck
- b) Tube coil over length
- c) Coil Bottom guide pin no room for movement
- d) Coil at cold condition no free movement
  - Insulator near gauge or flange.
  - Roof panel hole and guide pin hole not align
  - 'Donut' act as a lock at the bottom
  - At hot condition